

Published in final edited form as:

Cytotherapy. 2012 February ; 14(2): 223–231. doi:10.3109/14653249.2011.623690.

Myocardial improvement with human embryonic stem cell-derived cardiomyocytes enriched by p38MAPK inhibition

YEREM YEGHIAZARIANS^{1,2,*}, MEENAKSHI GAUR^{1,*}, YAN ZHANG¹, RICHARD E. SIEVERS¹,
CARISSA RITNER³, MEGHA PRASAD¹, ANDREW BOYLE^{1,2}, and HAROLD S.
BERNSTEIN^{2,3,4}

¹Department of Medicine, University of California, San Francisco, California, USA

²Eli and Edythe Broad Center of Regeneration Medicine and Stem Cell Research, University of California, San Francisco, California, USA

³Cardiovascular Research Institute, University of California, San Francisco, California, USA

⁴Department of Pediatrics, University of California, San Francisco, California, USA

Abstract

Background aims—We have shown previously that inhibition of the p38 mitogen-activated protein kinase (p38MAPK) directs the differentiation of human embryonic stem cell (hESC)-derived cardiomyocytes (hCM). We investigated the therapeutic benefits of intramyocardial injection of hCM differentiated from hESC by p38MAPK inhibition using closed-chest ultrasound-guided injection at a clinically relevant time post-myocardial infarction (MI) in a mouse model.

Methods—MI was induced in mice and the animals treated at day 3 with: (a) hCM, (b) human fetal fibroblasts (hFF) as cell control, or (c) medium control ($n = 10$ animals/group). Left ventricular ejection fraction (LVEF) was evaluated post-MI prior to therapy, and at days 28 and 60 post-cell therapy. Hearts were analyzed at day 60 for infarct size, angiogenesis, cell fate and teratoma formation.

Results—LVEF was improved in the hCM-treated animals compared with both hFF and medium control-treated animals at day 28 ($39.03 \pm 1.79\%$ versus $27.89 \pm 1.27\%$, $P < 0.05$, versus $32.90 \pm 1.46\%$, $P < 0.05$, respectively), with sustained benefit until day 60. hCM therapy resulted in significantly smaller scar size, increased capillary bed area, increased number of arterioles, less native cardiomyocyte (CM) apoptosis, and increased CM proliferation compared with the other two groups. These benefits were achieved despite a very low retention rate of the injected cells at day 60, as assessed by immunohistochemistry and quantitative real-time polymerase chain reaction (qPCR). Therapy with hCM did not result in intramyocardial teratoma formation at day 60.

Conclusions—This study demonstrates that hCM derived from p38MAPK-treated hESC have encouraging therapeutic potential.

© 2011 Informa Healthcare

Correspondence: **Harold S. Bernstein**, MD, PhD, University of California, 513 Parnassus Avenue, Box 1346, San Francisco, CA 94143–1346, USA. harold.bernstein@ucsf.edu. **Yerem Yeghiazarians**, MD, University of California, 505 Parnassus Avenue, Box 0103, San Francisco, CA 94143–0103, USA. yeghiza@medicine.ucsf.edu.

*These authors contributed equally to this work.

Disclosure of interest: The authors have no conflicts of interest, financial or otherwise, to disclose.

Keywords

cardiomyocyte; human embryonic stem cell; intra-myocardial injection; myocardial infarction; remodeling; teratoma

Introduction

Despite advances in the treatment of patients with cardiomyopathy and heart failure, there are currently no approaches in clinical practice that replace myocardial scar tissue with functioning contractile tissue (1–3). Therapeutic studies with adult stem cells and the mechanism of action of such cell therapies have yielded ambiguous results (4–9). Whether human embryonic stem cell (hESC)-derived cardiomyocytes (hCM) can survive in the ischemic environment after a myocardial infarction (MI) and improve cardiac function post-MI remains controversial.

One of the limitations in the use of hESC-derived hCM for therapeutic purposes is that these cardiac cells need to be generated in large numbers and with sufficient purity to avoid the formation of other tissues (10). Most groups have relied on spontaneous differentiation of hESC in the presence of serum (11,12). We have reported recently that treatment of hESC with a small molecule inhibitor of p38 mitogen-activated protein kinase (p38MAPK) during the stage of hESC differentiation that coincides with ectoderm/mesoendoderm divergence results in directed, accelerated differentiation of hCM, and that the resulting hCM maintain properties, such as genomic stability, that are essential for cell transplant therapy (13).

An additional limitation of pre-clinical small animal studies has been the difficulty of delivering cells to the infarcted heart at a clinically relevant time period within days after MI, because of increased animal mortality with a second open chest surgical procedure. We have recently developed an ultrasound-guided injection technique for use in a mouse MI model (14–16). This approach has allowed us to perform studies within a more clinically relevant timeframe by injecting cardiac cells into hearts several days post-MI without significant mortality, and has given us the ability to visualize more accurately and deliver cells into the peri-infarct border zone. We can also remove animals with unsuccessful injections (e.g. left ventricular cavity injection) from the study at the time of the injection to ensure uniform therapy in the groups studied.

In this report, we describe the therapeutic benefits of transthoracic intramyocardial injection of hCM derived by directed differentiation of hESC with a p38MAPK inhibitor. Using closed-chest ultrasound-guided injection, we compared the efficacy of hCM with human fetal fibroblasts and a medium control group in improving cardiac function post-MI. The therapy with hCM improved left ventricular ejection fraction (LVEF) compared with the other two groups at day 60 post-therapy, and resulted in a significantly smaller scar size, a larger capillary bed area and an increased number of arterioles. Interestingly, these benefits were achieved despite a very low retention rate of injected cells 2 months after therapy, as assessed by immunohistochemistry and quantitative real-time polymerase chain reaction (PCR). We also show that therapy with hCM produced in this manner did not result in myocardial teratoma formation.

Methods

Animals and study groups

Twelve-week-old female SCID-Beige (CB17SC-F C.B-Igh-1b/IcrTac-Prkdcscid; Taconic; Hudson, NY, USA) mice were used for all experiments. All animal studies were approved

by the University of California, San Francisco (UCSF; California, USA) Institutional Animal Care and Use Committee.

MI and echocardiography

MI was induced surgically by chronic ligation of the left anterior descending artery, as described previously (14–16). Echocardiography was performed under isoflurane anesthesia with the use of a Vevo660 (VisualSonics; Toronto, ON, Canada) equipped with a 30-MHz transducer. Echocardiograms were obtained at baseline, 2 days post-MI (before injection), and at days 28 and 60 post-MI (26 and 58 days post-injection). We measured LVEF, left ventricular end-systolic volume (ESV), left ventricular end-diastolic volume (EDV) and left ventricular wall thickness. Wall thickness was measured at the apical anterior wall (infarct wall thickness) and at the mid-anterior segment (peri-infarct wall thickness) separately on the parasternal long-axis view; posterior wall thickness was measured at the papillary muscle level. Three cycles were measured for each assessment and average values were reported. Echocardiographic analysis was performed in a blinded manner.

hESC differentiation and Percoll enrichment

All hESC studies were approved by the UCSF Human Gamete, Embryo and Stem Cell Research Committee. hESC were maintained and differentiated into hCM as described previously (13,17,18). Briefly, the previously described H9 hESC line, constitutively expressing enhanced green fluorescent protein (GFP) under control of the ubiquitin C promoter (17,19), was maintained on irradiated CF1 mouse embryonic fibroblasts (MEF). hESC were differentiated by human embryoid body (hEB) formation using differentiation medium [knock out-Dulbecco's Modified Eagle Medium (DMEM) medium containing 20% fetal bovine serum (FBS; SH 30070.03; Hyclone; Logan, UT, USA), 0.1 mM non-essential amino acids, 2 mM -glutamine and 0.1 mM 2-mercaptoethanol] as described previously (13,17,18). On day 7 following suspension culture, approximately 25 – 30 hEB/well were plated on 0.1% gelatin-coated 12-well plates in the same medium. Optimum conditions for treatment with the p38MAPK inhibitor, SB203580 (Calbiochem; Rockland, MA, USA), have been discussed elsewhere (13). hEB were treated in suspension culture with 10 μ M SB203580 from day 4 to day 6 of differentiation prior to replating on gelatin on day 7. We have described previously the phenotype and purity of hESC-derived hCM prepared using SB203580 (13). In brief, these are α -myosin heavy chain-, myosin light chain-4-, cardiac troponin T-expressing cells that contain nascent sarcomeres (by transmission electron microscopy) and demonstrate spontaneous contractile activity. On day 30, hEB were pre-treated with 10 μ M Rho-associated kinase inhibitor (Y-27632; Calbiochem) in differentiation medium overnight, following which hEB were dissociated using Blendzyme 4 (Roche; Nutley, NJ, USA) and enriched by Percoll-gradient centrifugation as described previously (12). The resulting enriched hCM were collected and further dissociated using Accutase (Sigma; Saint Louis, MO, USA) to generate single cells for injections using closed-chest ultrasound guided injection. This method achieved 90% viability, as assessed by trypan blue staining, after preparation as described and passage through a 50- μ L Hamilton syringe fitted with a sterile disposable 30-gauge needle, as used for ultrasound-guided injections (16).

Ultrasound-guided closed-chest injections

Human fetal skin fibroblasts (hFF; cell line CCL110; ATCC; Manassas, VA, USA) were cultured in modified Eagle's medium with Earl's Balanced Salt Solution (BSS) containing 10% FBS, 1 \times non-essential amino acids and 1 \times penicillin/streptomycin, as recommended by the provider. For injections, hFF were trypsinized and resuspended in differentiation medium. Animals underwent ultrasound-guided injection of hCM ($n = 10$), hFF ($n = 10$) or differentiation medium alone ($n = 10$), as described previously (13–16). All injected cells were suspended in the same differentiation medium used for the medium control injections

(i.e. knock out-DMEM, 20% FBS, 0.1 mM non-essential amino acids, 2 mM L-glutamine and 0.1 mM 2-mercaptoethanol). Each heart was injected at day 3 post-MI with 10^6 cells in 10 μ L differentiation medium or 10 μ L differentiation medium without cells, divided into two 5- μ L injections into the anterior wall. Intramyocardial delivery was observed in all animals, and none was removed from the study because of injection into the left ventricle (LV) cavity. Hearts destined for histologic staining were arrested in diastole by KCl injection, and perfusion-fixed with 10% buffered formalin before harvest at 60 days post-injection. Fixed specimens were embedded in paraffin and 5- μ m sections were analyzed by immunohistochemistry.

Tissue analysis

Tissue was analyzed in a blinded manner and the average of two analyzes was reported for each study in each animal. Heart tissue sections from each group were stained with hematoxylin and eosin and analyzed for the presence of teratomas, as described previously (13,17,18,20,21). Infarct size was measured by calculating the percentage circumferential extent of infarct zone as described previously (15). Sections from the mid-ventricular level were examined for blood vessel density and arteriole count by staining with anti-bodies against CD31 (Biocare, Concord, CA, USA) and α -smooth muscle actin (α SMA; Sigma-Aldrich; Saint Louis, MO, USA). Blood vessel density was analyzed using ImagePro software (MediaCybernetics; Bethesda, MD, USA) to detect the area of CD31 staining in the infarct zone (IZ), border zone (BZ) and remote myocardial zone (RZ). Arterioles defined as CD31⁺ vessels with an α SMA⁺ outer segment were counted manually in each region.

Sections from the mid-ventricular level were examined for the presence of cycling cardiomyocytes (CM) or (CM) undergoing apoptosis. Apoptosis was detected by terminal deoxynucleotidyl transferase dUTP nick end labeling (TUNEL) staining (ApopTag; Chemicon; Billerica, MA, USA). Cycling CM were detected using anti-Ki-67 (DAKO; Carpinteria, CA, USA). Apoptotic and cycling CM were quantified as the number of positive cells in five high-power fields examined for each of the relevant myocardial zones relative to the infarct (i.e. IZ, BZ and RZ).

Immunohistochemical detection of retained hCM

At day 60 post-MI, injected GFP⁺ hCM were detected by immunostaining using chicken anti-GFP (1:100) primary antibody (Aves Labs; Togard, OR, USA) followed by horseradish peroxidase-labeled goat anti-chicken secondary antibody (1:300; Aves Labs) and subsequent incubation with DAB reagent (Biocare; Concord, CA, USA). Antigen retrieval was performed by incubating sections with proteinase K. Negative staining controls lacking primary antibody were performed, as was control staining of tissue from mice from the medium-injected group. The fate of the grafted hCM was determined by indirect immunofluorescence staining of human cardiac troponin I (hcTnI). Sections were incubated with rabbit anti-hcTnI antibody (Abcam; Cambridge, MA, USA) following antigen retrieval by heat-induced epitope retrieval in sodium citrate, pH 6.0. Alexa 546-conjugated donkey anti-rabbit (Invitrogen; Carlsbad, CA, USA) was used for detection.

Quantitative real-time PCR analysis

For analysis of relative human cell concentration within mouse heart, RNA was isolated from total flash-frozen hearts with TRIzol (Invitrogen) using standard methods. To develop a standard expression curve, known numbers of hESC (50–250/mg) were added to normal heart samples prior to RNA isolation. cDNA was synthesized from isolated RNA using SuperScript III first-strand synthesis Super-Mix (Invitrogen) and quantitated using a Nanodrop ND-1000 Spectrophotometer (Nanodrop Technologies; Wilmington, DE, USA). Linear pre-amplification of target sequences was accomplished using the Applied

Biosystems PreAmp system according to the manufacturer's instructions. Relative expression was determined using TaqMan assays (Applied Biosystems; Carlsbad, CA, USA) on an ABI 7300 real-time PCR system with primers for human nuclear mitotic apparatus protein (Hs00272062_m1). Cycle times to detection were normalized against the reference gene glyceraldehyde 3-phosphate dehydrogenase (GAPDH) (4326317E), and relative changes were calculated using ABI version 1.4 sequence detection software. Relative expression values were adjusted for tissue mass.

Statistical analyzes

All analyzes (echocardiographic parameters, vessel counts, Ki67⁺ cell counts and quantitative real-time polymerase chain reaction (qPCR)) were performed using SPSS 11 (IBM; Armonk, NY, USA). For comparison between groups, ANOVA was used. For comparison within each group, a paired *t*-test with Bonferroni post-hoc test was used. A *P*-value of < 0.05 was considered significant for all studies.

Results

hCM reduced infarct size and resulted in improvement in cardiac function

To study the efficacy of hESC-derived hCM differentiated by p38MAPK inhibition, we induced MI in mice and injected animals at day 3 with hCM, hFF or control medium. We evaluated cardiac function at days 28 and 60 post-cell therapy, and infarct size at day 60 (Figure 1). To assess the effect of hCM transplant on infarct size, we evaluated histologic sections of infarcted myocardium 60 days post-MI. hCM-injected hearts showed significantly smaller infarct size at day 60 compared with hearts injected with hFF or medium vehicle ($0.15 \pm 0.07\%$ versus $0.25 \pm 0.51\%$ and $0.23 \pm 0.10\%$, respectively, $P = 0.008$; Figure 2).

To evaluate the effect of hCM therapy on cardiac function, we assessed left ventricular volumes, LVEF, and wall thicknesses at 28 and 60 days post-MI. There was less ventricular dilatation with hCM therapy compared with the hFF-injected group (ESV, 52.24 ± 9.85 versus 84.38 ± 25.84 μL , $P = 0.001$; EDV, 86.26 ± 11.16 versus 114.29 ± 25.35 μL , $P = 0.003$) at 60 days post-MI (Figure 3A). LVEF was uniformly reduced from an average of $50.5 \pm 1.3\%$ before MI to $36.1 \pm 2.2\%$ ($P < 0.0005$) at 2 days post-MI in all groups, with no significant differences amongst the groups (Figure 3B). At both the early (day 28) and late (60 days) time-points post-MI, LVEF improved significantly with injection of hCM versus hFF or medium (day 60, $39.7 \pm 3.7\%$ versus $27.1 \pm 6.4\%$, $P < 0.0001$, versus $32.7 \pm 2.6\%$, $P = 0.003$, respectively). Furthermore, there was significantly less peri-infarct wall thinning in the hCM-injected compared with hFF- and medium-injected groups (0.60 ± 0.08 mm versus 0.50 ± 0.04 mm, $P = 0.001$, versus 0.48 ± 0.04 mm, $P = 0.001$, respectively) (Figure 3C). There was no statistically significant difference in the posterior wall thickness; however, the infarct scar thickness was significantly greater with hCM therapy compared with the other two groups (0.37 ± 0.06 mm versus 0.25 ± 0.06 , $P < 0.001$, versus 0.28 ± 0.04 mm, $P = 0.002$, respectively) (Figure 3D), suggesting less tissue loss with hCM therapy.

hCM increased blood vessel density

To determine the effects of hCM transplantation on vascularization, we assessed capillary and arteriole density at day 60 post-MI. Sections from the midpapillary level were stained with antibodies against CD31 and αSMA . Therapy with hCM resulted in significant increases in vascularity after therapy (Figure 4). hCM increased the total vessel area in the BZ versus hFF and medium ($9 \pm 6\%$ versus $3 \pm 3\%$, $P < 0.03$, versus $3 \pm 1\%$, $P = 0.02$, respectively) (Figure 4A). Moreover, hCM therapy was associated with a significantly higher number of arterioles in the IZ (4.5 ± 3.3 versus 2.4 ± 1.1 , $P = 0.05$, versus 1.6 ± 0.8 ,

$P = 0.05$) and BZ (5.5 ± 2.9 versus 2.0 ± 0.9 , $P < 0.004$, versus 1.7 ± 1.1 , $P = 0.008$) compared with hFF and medium, respectively (Figure 4B). Vessel counts did not differ between any groups in the RZ.

Cardiomyocyte apoptosis and proliferation after therapy

To evaluate the effects of hCM therapy on CM cell death and proliferation, we examined histologic sections of myocardium at day 60 post-MI for cells expressing TUNEL antigens and Ki67, respectively. At day 60 post-MI, hCM treatment resulted in reduction in the number of apoptotic CM at the BZ (0.37 ± 0.14 versus 0.57 ± 0.14 , $P < 0.008$, versus 0.66 ± 0.10 , $P < 0.008$, respectively) (Figure 5A). This was consistent with the increased wall thickness near the infarct scar seen with hCM therapy (Figure 3D). To evaluate whether hCM therapy affected proliferation of host CM, we counted the number of cycling host CM and found that hCM therapy resulted in an increase in the number of Ki67⁺ CM nuclei compared with hFF and medium therapies (1.76 ± 0.97 versus 0.72 ± 1.1 , $P = 0.012$, versus 0.86 ± 0.25 , $P = 0.015$, respectively) (Figure 5B).

Fate of implanted hCM

As other studies have shown very low engraftment rates for stem cell-derived hCM, we investigated the fate of implanted cells at early and late time-points. Immunohistochemical evaluation of tissue sections at both the injection sites and throughout the recipient hearts showed few retained GFP⁺ (Figure 6A,B) or hcTnI⁺ (Figure 6C,D) hCM at day 60. Given the low number of residual hESC-derived cells, we used real-time PCR to quantitate cell retention over time (Figure 6E). This analysis showed that fewer than 250 hESC-derived CM/mg heart tissue remained at day 7 post-transplant, and that there was no detectable hCM at 14 days. We also examined hearts for hESC-derived vascular cells; however, no GFP⁺ smooth muscle actin (SMA⁺) or GFP⁺ CD31⁺ cells were detected by immunohistochemistry at day 60 (data not shown). Detailed analysis of hematoxylin and eosin-stained sections showed no evidence of teratoma formation in any of the experimental groups.

Discussion

The major findings of this study are: (a) hESC-derived hCM obtained through p38MAPK kinase inhibitor-directed differentiation, and purified by Percoll-gradient centrifugation, confer functional benefit when transplanted into injured mouse myocardium; (b) ultrasound-guided injections of hCM into mouse hearts 3 days post-MI results in improvement of cardiac function, smaller infarct size, less deleterious LV remodeling, and an increase in the peri-infarct and scar wall thickness at day 60 post-therapy compared with injection of hFF or medium; (c) treatment with hCM results in an increase in capillary bed area and an increase in arteriole number compared with treatment with hFF or medium; (d) hCM therapy results in a decrease in native cardiomyocyte apoptosis and an increase in CM proliferation; (e) these benefits are achieved despite a low retention rate of hCM in the myocardium and without cell differentiation after therapy at day 60, suggesting a predominantly paracrine mechanism; (f) hCM therapy is safe and does not result in teratoma formation at 60 days of follow-up in the immunodeficient mouse model; (g) human fetal fibroblast therapy does not result in cardiac functional improvement post-MI in this model. While our group and others had previously demonstrated enrichment of hESC-derived hCM with p38MAPK inhibition (13,22), the effectiveness of these cells *in vivo* has not been studied until now. In addition, other groups have examined the potential therapeutic benefits of hESC-derived hCM in rodent models of MI (23–28); however, they did not evaluate hCM specifically derived by p38MAPK inhibition. As the proposed mechanism by which p38MAPK inhibition preferentially directs mesodermal differentiation at the expense of ectoderm (13) differs

from other methods for directed differentiation of hCM (23,29), it was not obvious that these cells would behave similarly to other hESC-derived cardiac cells *in vivo*.

Our results demonstrate that injection of hCM attenuates adverse left ventricular remodeling and improves cardiac function compared with hFF and control medium. The benefits are achieved despite a low myocardial retention rate of the cells. These findings are reminiscent of studies with adult bone marrow cells, where significant functional improvement was achieved post-MI despite a low retention rate of the transplanted cells (15). In contrast with adult stem cells, we hypothesized that hCM would result in higher cell retention and differentiation, but this was not seen. Despite low cell retention, however, treatment with hCM resulted in an increase in capillary bed area and an increase in arteriole number compared with treatment with hFF or stem cell differentiation medium. In addition to the beneficial effects on blood vessel numbers, hCM treatment resulted in a decrease in native CM apoptosis and an appreciable increase in the proliferation of these cells. In contrast with some studies that have shown an initial functional benefit followed by a fall-off in this benefit over time (25), the improvement in cardiac function seen in this study at the early time-point (day 28) persisted through the entire study (60 days post-MI).

Other groups citing evidence of low engraftment with other sources of cardiac stem cells have proposed paracrine mechanisms that include recruitment of resident cardiac stem cells (30,31), inhibition of fibrosis (32), cardioprotection (probably through secretion of hepatocyte growth factor (HGF), transforming growth factor (TGF)- β , vascular endothelial growth factor (VEGF), insulin-like growth factor (IGF)-1, stanniocalcin 1, and granulocyte-macrophage colony-stimulating factor (GM-CSF)) and promotion of neoangiogenesis (33). Another hypothesis is that hCM may modulate the inflammatory microenvironment of ischemic tissue. Our data showing smaller infarct size and an increase in peri-infarct wall thickness (Figures 2C and 3C), and an increase in capillary bed area and arteriole number (Figure 4), suggest that paracrine effects leading to inhibition of fibrosis and neoangiogenesis, respectively, are probably responsible for the functional effects observed in our studies.

Over the past few years, several studies have reported improvement in cardiac function with transplantation of cardiomyocytes or cardiac progenitor cells derived from hESC (23,26,28,29,34–36). The majority of injected cells in these reports disappeared within days after transplantation. The goal of this study was to test whether a new method for differentiation (i.e. p38MAPK inhibition) and the mode of delivery (i.e. ultrasound-guided closed-chest several days after MI) might lead to better engraftment and therefore a greater functional benefit. While a higher rate of engraftment and larger measurable improvement in function were not observed, our experiments show that effects similar to those seen with spontaneously differentiated hCM can be achieved with hCM obtained using a directed differentiation method shown previously by us and others to improve the yield of hCM *in vitro* (13,22). These data also suggest that open-heart delivery immediately following infarct may not be necessary to achieve previously seen desired effects with hESC-derived hCM.

Undifferentiated hESC produce germ-line tumors, or teratomas, when introduced into a physiologic environment (21). As such, methods that either produce highly purified cardiac cells derived from hESC, or eliminate undifferentiated cells (20), are critical to avoiding teratoma formation. With the isolation method described in this report, it is encouraging that we did not detect teratomas in the heart. It should be noted that, in this rodent study, we transplanted human cells into an immunodeficient mouse model. Further investigation is required to evaluate whether hESC would result in teratoma formation when transplanted into immunosuppressed recipients.

In summary, we report that highly purified hCM can be obtained for therapeutic purposes by directed differentiation of hESC into hCM with p38MAPK inhibition, and subsequent purification by Percoll-gradient centrifugation, and that these cells improve cardiac function post-MI and result in significantly smaller scar size, higher capillary density and increased numbers of arterioles, even when introduced by closed-chest injection. These benefits were achieved despite a very low cell retention rate at 60 days post-therapy, as assessed by quantitative PCR and immunohistochemistry. These studies also confirm that therapy with hCM produced and delivered in this manner does not result in teratoma formation.

Acknowledgments

The authors thank Walter Liszewski for assistance with cell culture, and members of the Bernstein and Yeghiazarians laboratories for helpful discussion. This work was supported by funds from the UCSF Cardiac Stem Cell Foundation to YY, and a Comprehensive Research Grant from the California Institute for Regenerative Medicine (RC1-00104), a Public Health Service Grant from NHLBI (HL085377), and a gift from the Polin Foundation to HSB.

References

1. Losordo DW, Dimmeler S. Therapeutic angiogenesis and vasculogenesis for ischemic disease. II. Cell-based therapies. *Circulation*. 2004; 109:2692–7. [PubMed: 15184293]
2. Wollert KC, Drexler H. Clinical applications of stem cells for the heart. *Circ Res*. 2005; 96:151–63. [PubMed: 15692093]
3. Rosenzweig A. Cardiac cell therapy: mixed results from mixed cells. *N Engl J Med*. 2006; 355:1274–7. [PubMed: 16990391]
4. Balsam LB, Wagers AJ, Christensen JL, Kofidis T, Weissman IL, Robbins RC. Haematopoietic stem cells adopt mature haematopoietic fates in ischaemic myocardium. *Nature*. 2004; 428:668–73. [PubMed: 15034594]
5. Jackson KA, Majka SM, Wang H, Pocius J, Hartley CJ, Majesky MW, et al. Regeneration of ischemic cardiac muscle and vascular endothelium by adult stem cells. *J Clin Invest*. 2001; 107:1395–402. [PubMed: 11390421]
6. Janssens S, Theunissen K, Boogaerts M, Van de Werf F. Bone marrow cell transfer in acute myocardial infarction. *Nat Clin Pract Cardiovasc Med*. 2006; 3(Suppl 1):S69–72. [PubMed: 16501635]
7. Kocher AA, Schuster MD, Szabolcs MJ, Takuma S, Burkhoff D, Wang J, et al. Neovascularization of ischemic myocardium by human bone-marrow-derived angioblasts prevents cardiomyocyte apoptosis, reduces remodeling and improves cardiac function. *Nat Med*. 2001; 7:430–6. [PubMed: 11283669]
8. Murry CE, Soonpaa MH, Reinecke H, Nakajima H, Nakajima HO, Rubart M, et al. Haematopoietic stem cells do not transdifferentiate into cardiac myocytes in myocardial infarcts. *Nature*. 2004; 428:664–8. [PubMed: 15034593]
9. Orlic D, Kajstura J, Chimenti S, Limana F, Jakoniuk I, Quaini F, et al. Mobilized bone marrow cells repair the infarcted heart, improving function and survival. *Proc Natl Acad Sci USA*. 2001; 98:10344–9. [PubMed: 11504914]
10. Wong SS, Bernstein HS. Cardiac regeneration using human embryonic stem cells: producing cells for future therapy. *Regen Med*. 2010; 5:763–75. [PubMed: 20868331]
11. Kehat I, Kenyagin-Karsenti D, Snir M, Segev H, Amit M, Gepstein A, et al. Human embryonic stem cells can differentiate into myocytes with structural and functional properties of cardiomyocytes. *J Clin Invest*. 2001; 108:407–14. [PubMed: 11489934]
12. Xu C, Police S, Rao N, Carpenter MK. Characterization and enrichment of cardiomyocytes derived from human embryonic stem cells. *Circ Res*. 2002; 91:501–8. [PubMed: 12242268]
13. Gaur M, Ritner C, Sievers R, Pedersen A, Prasad M, Bernstein HS, et al. Timed inhibition of p38MAPK directs accelerated differentiation of human embryonic stem cells into cardiomyocytes. *Cytotherapy*. 2010; 12:807–17. [PubMed: 20586669]

14. Zhang Y, Takagawa J, Sievers RE, Khan MF, Viswanathan MN, Springer ML, et al. Validation of the wall motion score and myocardial performance indexes as novel techniques to assess cardiac function in mice after myocardial infarction. *Am J Physiol Heart Circ Physiol.* 2007; 292:H1187–92. [PubMed: 17028161]
15. Yeghiazarians Y, Zhang Y, Prasad M, Shih H, Saini SA, Takagawa J, et al. Injection of bone marrow cell extract into infarcted hearts results in functional improvement comparable to intact cell therapy. *Mol Ther.* 2009; 17:1250–6. [PubMed: 19384293]
16. Springer ML, Sievers RE, Viswanathan MN, Yee MS, Foster E, Grossman W, et al. Closed-chest cell injections into mouse myocardium guided by high-resolution echocardiography. *Am J Physiol Heart Circ Physiol.* 2005; 289:H1307–14. [PubMed: 15908468]
17. King FW, Ritner C, Liszewski W, Kwan HC, Pedersen A, Leavitt AD, et al. Subpopulations of human embryonic stem cells with distinct tissue-specific fates can be selected from pluripotent cultures. *Stem Cells Dev.* 2009; 18:1441–50. [PubMed: 19254177]
18. Ritner C, Wong SS, King FW, Mihardja SS, Liszewski W, Erle DJ, et al. An engineered cardiac reporter cell line identifies human embryonic stem cell-derived myocardial precursors. *PLoS One.* 2011; 6:e16004. [PubMed: 21245908]
19. Nicholas CR, Gaur M, Wang S, Pera RA, Leavitt AD. A method for single-cell sorting and expansion of genetically modified human embryonic stem cells. *Stem Cells Dev.* 2007; 16:109–17. [PubMed: 17348809]
20. King FW, Liszewski W, Ritner C, Bernstein HS. High-throughput tracking of pluripotent human embryonic stem cells with dual fluorescence resonance energy transfer molecular beacons. *Stem Cells Dev.* 2011; 20:475–84. [PubMed: 20624034]
21. Ritner C, Bernstein HS. Fate mapping of human embryonic stem cells by teratoma formation. *J Vis Exp.* 2010:2036.
22. Graichen R, Xu X, Braam SR, Balakrishnan T, Norfiza S, Sieh S, et al. Enhanced cardiomyogenesis of human embryonic stem cells by a small molecular inhibitor of p38 MAPK. *Differentiation.* 2008; 76:357–70. [PubMed: 18021257]
23. van Laake LW, Passier R, Monshouwer-Kloots J, Verkleij AJ, Lips DJ, Freund C, et al. Human embryonic stem cell-derived cardiomyocytes survive and mature in the mouse heart and transiently improve function after myocardial infarction. *Stem Cell Res.* 2007; 1:9–24. [PubMed: 19383383]
24. van Laake LW, Passier R, Monshouwer-Kloots J, Nederhoff MG, Ward-van Oostwaard D, Field LJ, et al. Monitoring of cell therapy and assessment of cardiac function using magnetic resonance imaging in a mouse model of myocardial infarction. *Nat Protoc.* 2007; 2:2551–67. [PubMed: 17947998]
25. van Laake LW, Passier R, Doevendans PA, Mummery CL. Human embryonic stem cell-derived cardiomyocytes and cardiac repair in rodents. *Circ Res.* 2008; 102:1008–10. [PubMed: 18436793]
26. Leor J, Gerecht S, Cohen S, Miller L, Holbova R, Ziskind A, et al. Human embryonic stem cell transplantation to repair the infarcted myocardium. *Heart.* 2007; 93:1278–84. [PubMed: 17566061]
27. Kofidis T, Lebl DR, Swijnenburg RJ, Greeve JM, Klima U, Robbins RC. Allopurinol/uricase and ibuprofen enhance engraftment of cardiomyocyte-enriched human embryonic stem cells and improve cardiac function following myocardial injury. *Eur J Cardiothorac Surg.* 2006; 29:50–5. [PubMed: 16337396]
28. Caspi O, Huber I, Kehat I, Habib M, Arbel G, Gepstein A, et al. Transplantation of human embryonic stem cell-derived cardiomyocytes improves myocardial performance in infarcted rat hearts. *J Am Coll Cardiol.* 2007; 50:1884–93. [PubMed: 17980256]
29. Laflamme MA, Chen KY, Naumova AV, Muskheli V, Fugate JA, Dupras SK, et al. Cardiomyocytes derived from human embryonic stem cells in pro-survival factors enhance function of infarcted rat hearts. *Nat Biotechnol.* 2007; 25:1015–24. [PubMed: 17721512]
30. Nakanishi C, Yamagishi M, Yamahara K, Hagino I, Mori H, Sawa Y, et al. Activation of cardiac progenitor cells through paracrine effects of mesenchymal stem cells. *Biochem Biophys Res Commun.* 2008; 374:11–6. [PubMed: 18586003]

31. Loffredo FS, Steinhauser ML, Gannon J, Lee RT. Bone marrow-derived cell therapy stimulates endogenous cardiomyocyte progenitors and promotes cardiac repair. *Cell Stem Cell*. 2011; 8:389–98. [PubMed: 21474103]
32. Ohnishi S, Sumiyoshi H, Kitamura S, Nagaya N. Mesenchymal stem cells attenuate cardiac fibroblast proliferation and collagen synthesis through paracrine actions. *FEBS Lett*. 2007; 581:3961–6. [PubMed: 17662720]
33. Takahashi M, Li TS, Suzuki R, Kobayashi T, Ito H, Ikeda Y, et al. Cytokines produced by bone marrow cells can contribute to functional improvement of the infarcted heart by protecting cardiomyocytes from ischemic injury. *Am J Physiol Heart Circ Physiol*. 2006; 291:H886–93. [PubMed: 16603697]
34. Yang L, Soonpaa MH, Adler ED, Roepke TK, Kattman SJ, Kennedy M, et al. Human cardiovascular progenitor cells develop from a KDR⁺ embryonic stem cell-derived population. *Nature*. 2008; 453:524–8. [PubMed: 18432194]
35. Rubart M, Field LJ. Stem cell differentiation: cardiac repair. *Cells Tissues Organs*. 2008; 188:202–11. [PubMed: 18160823]
36. Yoshida Y, Yamanaka S. Recent stem cell advances: induced pluripotent stem cells for disease modeling and stem cell-based regeneration. *Circulation*. 2010; 122:80–7. [PubMed: 20606130]

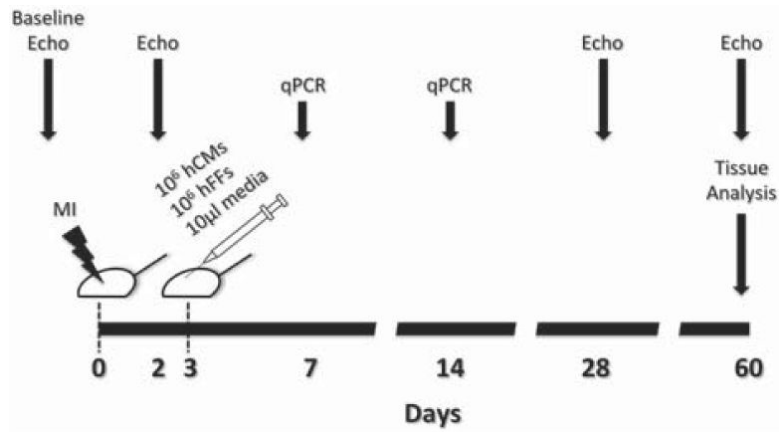


Figure 1. Schematic representation of the experimental plan. Details discussed in the text.

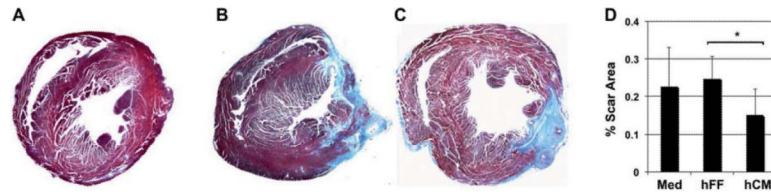


Figure 2. Limitation of infarct size with hCM transplant. (A–C) Histologic sections of hearts at the level of the mid-papillary muscles stained with Masson's trichrome to indicate scar tissue (blue) at 60 days post-MI. Typical examples of normal (A) and post-MI hearts injected with medium (B) or hCM (C) are shown. (D) Infarct size was determined by morphometry. Injection of hCM significantly reduced the scar area compared with hFF injection. Medium (Med) injection was performed as a control. Data shown are mean \pm SD ($n = 5$). $*P = 0.008$.

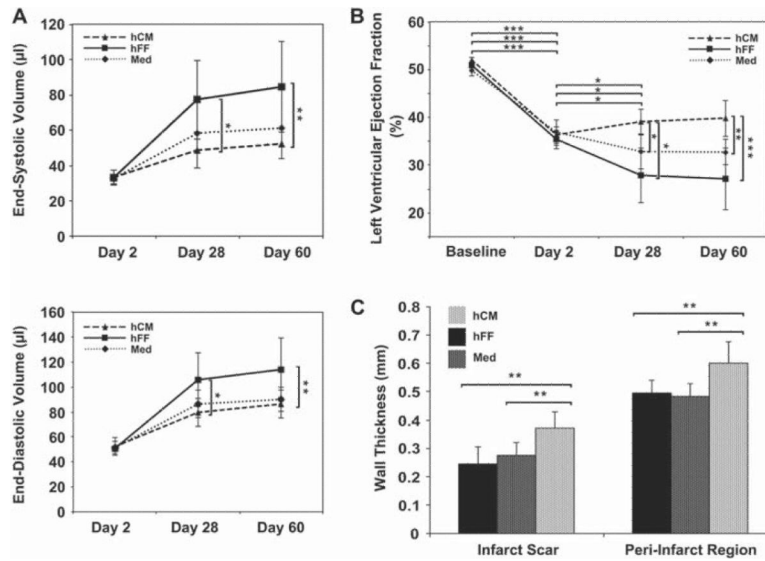


Figure 3. Functional improvement with hCM transplant. (A) End-systolic (upper) and end-diastolic (lower) volumes were measured over time in hearts injected with hCM, hFF or control medium (Med). Hearts injected with hCM post-MI showed sustained decreases in volumes over time, with less evidence of dilated cardiomyopathy. (B) LVEF was assessed at baseline (pre-MI) and at the same time-points as in (A). Hearts injected with hCM post-MI showed an improvement in LVEF that was sustained over time. (C) Wall thickness of the peri-infarct region and the infarct scar was measured echocardiographically at day 60 post-MI. For all panels, data shown are mean \pm SD (hCM, $n = 7$; hFF, $n = 5$; Med, $n = 9$). * $P < 0.05$; ** $P < 0.005$; *** $P < 0.0005$.

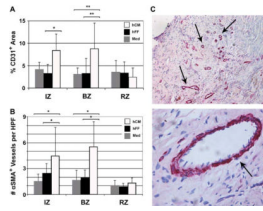


Figure 4. Enhanced vascularity with hCM transplant. hCM resulted in both increased CD31⁺ vessels (A) and number of α SMA⁺ arterioles (B) in the IZ and BZ. HPF, high-power field (40 \times magnification). Data shown are mean \pm SD (hCM, $n = 10$; hFF, $n = 7$; Med, $n = 4$). * $P < 0.05$; ** $P < 0.01$. (C) Typical sections with α SMA⁺ arterioles indicated by arrows (upper, 10 \times magnification; lower, 40 \times magnification).

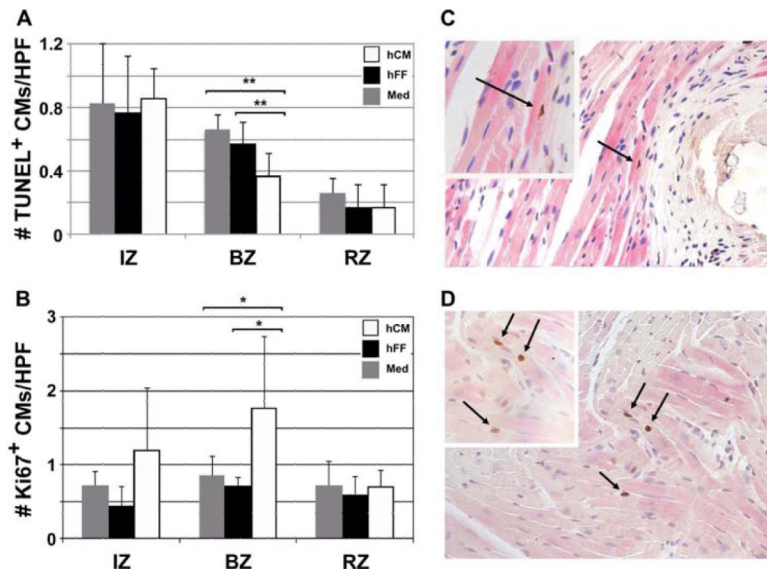


Figure 5.

Reduced CM apoptosis and increased CM proliferation with hCM transplant. (A) hCM therapy resulted in a significant reduction in the number of TUNEL⁺ apoptotic CM at the BZ on day 60 post-MI. HPF, 40 × magnification. Data shown are mean ± SD ($n = 5$). $**P < 0.01$. (B) hCM-injected hearts showed an increase in the number of cardiac Troponin I (cTnI⁺) Ki67⁺ proliferating CM at the BZ on day 60 post-MI. HPF, 40 × magnification. Data shown are mean ± SD ($n = 5$). $*P < 0.02$. (C) Typical low-power field (20 × magnification) showing TUNEL⁺ apoptotic nucleus (dark blue; arrows). Inset, 40 × magnification. (D) Typical low-power field (20 × magnification) showing Ki67⁺ (brown) proliferating nuclei (arrows) in cTnI⁺ (pink striated) CM.

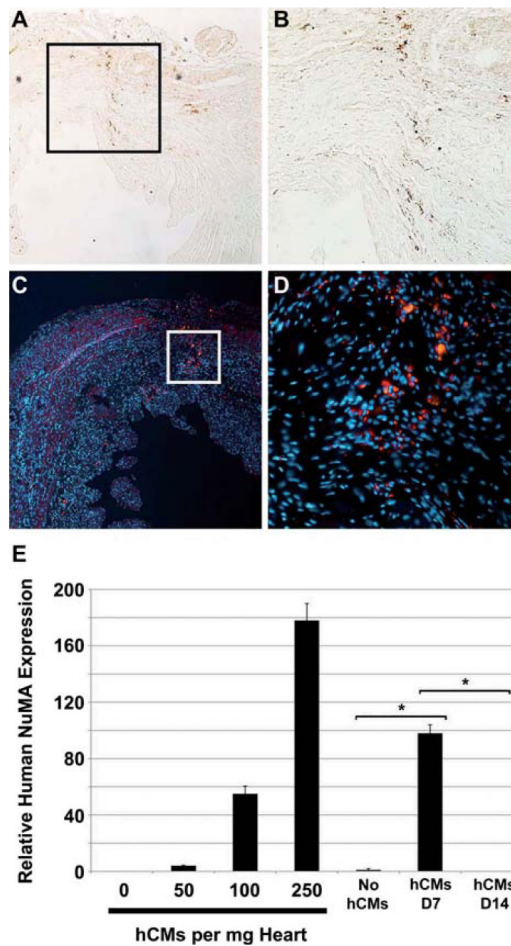


Figure 6.

Transplanted hCM do not persist in mouse hearts. (A–D) Immunohistochemical analysis demonstrated rare residual GFP⁺ or hcTnI⁺ cells at 60 days post-MI. GFP was detected by indirect immunohistochemistry (A, B; brown) and hcTnI by indirect immunofluorescence (C, D; red). Nuclei were stained with DAPI (blue) in indirect immunofluorescence (C, D) images. (A, C) Typical low-power fields (10 × magnification) are shown. (B) Higher magnification (20 ×) of boxed area in (A). (D) Higher magnification (40 ×) of boxed area in (C). (E) The presence of residual hESC-derived CM was assessed by quantitative PCR using primer sets against human nuclear mitotic antigen (NuMA). As few as 50 hCM/mg heart tissue could be detected in control samples. While fewer than 250 hCM/mg remained at day 7 (D7) post-transplant, there was no detectable signal for human NuMA in transplanted hearts at 14 days post-cell transplant. The rare residual cells shown in (A–D) were apparently beneath the limit of detection by PCR. Data shown are mean ± SEM ($n = 3$). * $P < 0.001$.